Unraveling energy homeostasis in a dynamic model of glycolysis in *Escherichia coli*

Giulia Giordano[1], Lotte M. de Graaf[2], Eleni Vasilakou[2], and S. Aljoscha Wahl[2]

***Abstract*— We study dynamic metabolic models that describe the cellular responses of microorganisms under changing environmental conditions, such as substrate perturbations. Feast-famine experiments in *Escherichia coli* show that, despite the enormous extracellular perturbations, important quantities such as the cell energy charge remain practically constant. We propose a simplified kinetic model of glycolysis in *E. coli* and we analyse it to investigate the mechanisms that guarantee the observed homeostatic energy charge. Identifying the source of this extraordinary robustness will streamline the synthesis of robust and efficient "cell factories" for the production of relevant chemicals, enabling sustainable processes.**

I. Introduction

Microbial cells are constantly exposed to dynamic environmental conditions: changing temperatures as well as nutrient supply varying in time are found in many ecosystems. However, microbial cells appear to be robust [1], [3], [19], [25], [27] towards many perturbations, including very fast changes. How this robustness is generated from kinetic and stoichiometric properties of the metabolic network has not been fully elucidated. Biological systems are inherently *noisy*, with large variations in enzyme expression levels from cell to cell and putative genetic mutations [29], hence metabolic fitness should be robust towards external as well as internal perturbations [18].

Analysing microbial metabolism under dynamic conditions is important not only to understand the source of the observed astounding robustness, but also to enable control and optimisation of processes in large-scale bioreactors. In fact, for better efficiency, processes are performed at very large scale. Large-scale bioreactors have long mixing times, leading to inhomogeneities: there are zones of high and (very) low substrate concentration [20]. A cell travels through these zones and experiences phases of high and low nutrient concentrations. To study the cellular response to these conditions in laboratory-scale bioreactors (which are much cheaper to operate, and allow for easy manipulation and simple sampling of biomass for metabolomics and proteomics), a scale-down approach must be adopted: nutrient gradients experienced by the cell are mimicked using a *periodic feeding regime*, leading to repetitive profiles of high and low concentrations, known as *feast-famine perturbations*. Note that the famine phase is kept short enough to make sure that no cell-death phenomena occur.

The cellular responses of microorganisms in dynamic environments have been studied in various organisms, taking into account different operating conditions. The impact of dynamic conditions seems to be very organism-specific. For *E. coli*, experiments both with cultures cultivated under steady conditions and then perturbed by a substrate pulse [21] and with cultures constantly exposed to dynamic environmental conditions [32] reveal that metabolic fluxes and the concentrations of central metabolites change significantly; the uptake rate varies more than 10-fold within seconds. In the experiments with repetitive perturbations, biomass and product yields are reduced compared to steady environmental conditions. Despite the dynamic changes in fluxes and concentrations, the *cellular energy charge* $\frac{[ATP]+0.5[ADP]}{[ATP]+[ADP]+[AMP]}$, where ATP, ADP and AMP are the molecules governing energy flows within the cell [10], stays within very close boundaries, between 0.7 and 0.85: its value is approximately the same as in steady environmental conditions. ATP is consumed and produced in many metabolic pathways, with rapidly changing fluxes; although the turnover is high, the concentration is practically constant. These mechanisms seem related to energy drains [28], but the robustness allowing for energy homeostasis is not yet fully understood.

In this paper, the fundamental question of robust function in the presence of perturbations is approached for glycolysis in *Escherichia coli* [12]. In particular, Section II proposes a new simple model of glycolysis in *E. coli*, based on the chemical reactions reported in [22], [31]. Our goal is to build a simple model that, differently from the famous one proposed in [12], can capture the essence of the dynamics while using the *smallest possible* number of variables. The corresponding dynamical system is analysed to prove its positivity and robustness, and the existence of a steady state that, under suitable assumptions, is unique. The system is also shown to be a candidate oscillator [5], [6], consistently with glycolytic oscillations reported in the literature, not only for yeast [2], [11], but also for *E. coli* [22], [23], [31] and even for human pancreatic beta-cells [33]. The steady-state influences among the system variables (i.e., the variations in the steady state of a variable due to a persistent positive perturbation added to the differential equation of another variable) are also assessed [9], [14], [15], to reveal influences whose sign is preserved regardless of the parameters, and to analyse sensitivity to parameter variations; it turns out that the variation of $[ATP]$ due to additive perturbations affecting

This research is partially supported by the BioDate 2018 grant *Robustness by design? Structural analysis of dynamic metabolic models*, awarded to G.G. and S.A.W. by the Delft Bioengineering Institute, and by the Aspasia grant and the DTF grant awarded to G.G.

[1]Delft Center for Systems and Control, Delft University of Technology, The Netherlands. G.Giordano@tudelft.nl

[2]Department of Biotechnology, Delft University of Technology, The Netherlands. L.M.deGraaf@student.tudelft.nl, {E.Vasilakou,S.A.Wahl}@tudelft.nl

$$
\begin{aligned}
\dot{x}_1 &= u_{GLC}^{feed} - k_1 c_x f_1(x_1, x_4) - D x_1 \\
\dot{x}_2 &= f_1(x_1, x_4) - f_2(x_2, x_5) - \mu x_2 \\
\dot{x}_3 &= f_2(x_2, x_5) - h_3(x_3, x_5) + f_3(x_4, x_5) - g_3(x_3) - \mu x_3 \\
\dot{x}_4 &= -f_1(x_1, x_4) + 2h_3(x_3, x_5) - 2f_3(x_4, x_5) - h_4(x_4, x_5) - \mu x_4 \\
\dot{x}_5 &= -f_2(x_2, x_5) + 2h_3(x_3, x_5) - 2f_3(x_4, x_5) + h_4(x_4, x_5) - g_5(x_5) - \mu x_5
\end{aligned}
$$

TABLE I: The dynamical system modelling glycolysis in *E. coli*.

the other metabolites is particularly small, which supports the evidence of energy homeostasis (Section III). Finally, the theoretical predictions obtained with the proposed model are compared to experimental observations from *E. coli* cultivations: the model is able to reproduce very well the qualitative evolution of concentrations over time, and the observed energy homeostasis (Section IV).

II. Glycolysis in *E. coli*: a Simple Dynamic Model

We propose and analyse here a simple ordinary-differential-equation model that captures the dynamics of glycolysis in *E. coli*, based on [22], [31]. The state variables of the dynamic model are the concentrations of the species: extracellular glucose, $x_1 = [GLC_{EC}]$; fructose 6-phosphate, $x_2 = [F6P]$; fructose 1,6-bisphosphate, $x_3 = [FDP]$; 2-phosphoenolpyruvate, $x_4 = [PEP]$; adenosine triphosphate, $x_5 = [ATP]$. Other species involved are ADP (adenosine diphosphate), AMP (adenosine monophosphate), PYR (pyruvate). The considered chemical reactions are:

$$
\begin{aligned}
GLC + PEP &\xrightarrow{f_1(x_1, x_4)} F6P + PYR \\
F6P + ATP &\xrightarrow{f_2(x_2, x_5)} FDP + ADP \\
FDP + 2ADP &\underset{f_3(x_3, x_5)}{\overset{h_3(x_3, x_5)}{\rightleftharpoons}} 2PEP + 2ATP \\
FDP &\xrightarrow{g_3(x_3)} \emptyset \\
PEP + ADP + H &\xrightarrow{h_4(x_4, x_5)} PYR + ATP \\
ATP &\xrightarrow{g_5(x_5)} ADP
\end{aligned}
$$

where f_i, g_i and h_i are the reaction rate functions. This list of reactions relies on simplifications suggested by experimental evidence: many other reactions occur within the glycolysis pathway, but they are either lumped (several intermediate steps are replaced by an overall reaction) or considered at equilibrium in view of their rapidity due to high enzyme capacity. The consumption of FDP due to the reaction $FDP \xrightarrow{g_3} \emptyset$ implicitly represents the conversion of $G6P$ (glucose-6-phosphate) and ATP into glycogen, not explicitly considered in the model. Also the reaction $2ADP \rightleftharpoons ATP + AMP$ occurs, but it is extremely fast, hence it can be assumed at equilibrium and replaced by the equality

$$[ATP][AMP] = [ADP]^2. \tag{1}$$

The total concentration of adenine nucleotides changes extremely slowly, hence can be legitimately assumed constant:

$$[ATP] + [ADP] + [AMP] = c_{AxP}, \tag{2}$$

where $c_{AxP} = 10.7$ mmol/L$_{IC}$ (cf. [30]); we denote by L$_{IC}$ the measure unit for intracellular (cytosol) volume and by L$_{EC}$ the measure unit for extracellular (culture) volume.

Considering the glucose feeding input u_{GLC}^{feed}, the dilution rate D and the specific growth rate μ, the resulting dynamical system that describes the time evolution of species concentrations is reported in Table I, where $c_x = 0.0154$ L$_{IC}$/L$_{EC}$ and k_1 are positive constants. Assuming that dilution and growth (averaged over each feast-famine cycle) are the same, hence the biomass concentration is constant, we set $\mu = D$.

Assumption 1: Functions f_i, g_i and h_i are nonnegative. Functions f_i are increasing and asymptotically bounded in each argument, and zero when at least one argument is zero. Functions g_i are increasing and asymptotically unbounded, and zero when their argument is zero. Functions h_i are increasing and asymptotically bounded in the first argument, and decreasing and asymptotically zero in the second; they are zero when the first argument is zero, and strictly positive (finite) when only the second argument is zero. ◇

Typically, functions f_i are Michaelis-Menten or Hill functions, while functions g_i are linear (mass action kinetics).

A. Positivity, boundedness and existence of a steady-state

Since the state variables represent concentrations of chemical species, they should remain nonnegative (when the initial conditions are nonnegative) and finite throughout the system evolution. The proposed model is able to reproduce this behaviour, as proven next.

Proposition 1: Under Assumption 1, the dynamical system in Table I:
(i) is positive (the nonnegative orthant is an invariant set);
(ii) has solutions that are globally asymptotically bounded in the set $\mathcal{B} = \{x : 0 \le x_i \le x_i^{max}, i = 1, \dots, 5\}$, where $x_i^{max} > 0$ are suitable constants, for all nonnegative initial conditions;
(iii) has a steady state $\bar{x}$, which is nonzero if $u_{GLC}^{feed} > 0$. □

Proof: (i) Positivity of the system is guaranteed since, when $x_i = 0$, the corresponding equation $\dot{x}_i$ has only nonnegative terms in its right-hand side, hence x_i can no longer decrease. (ii) Boundedness follows from the observation that, since functions f_i and h_i are bounded, the nonpositive terms ($-g_i$ and/or $-Dx_1$, $-\mu x_i$) dominate in the equation $\dot{x}_i$ when x_i is sufficiently large. (iii) Boundedness ensures that the system admits at least one steady state $\bar{x} \in \mathcal{B}$ [24], [26]. Since $\bar{x}_1$ cannot be zero if $u_{GLC}^{feed} > 0$, it must be $\bar{x} \neq 0$. ■

If the dilution rate is $D \neq 0$ and the specific growth rate is $\mu \neq 0$, it is possible to have a steady state whose components are all zero but the first: $\bar{x}_2 = 0$ implies $\bar{x}_4 = 0$, implying in

turn $\bar{x}_3 = 0$ and $\bar{x}_5 = 0$, while $\bar{x}_1 = u_{GLC}^{feed}/D$. Conversely, if $D = \mu = 0$, then $\bar{x}_1$ and $\bar{x}_4$ cannot be zero, hence $\bar{x}_2$ and $\bar{x}_5$ cannot be zero, thus $\bar{x}_3$ cannot be zero: therefore, $\bar{x} > 0$ componentwise.

B. Uniqueness of the steady state

We show that, for any fixed value of the feeding input u_{GLC}^{feed}, the system admits a unique steady-state.

In view of the monotonicity properties of the reaction rate functions, according to Assumption 1, their derivatives can be denoted as: $\partial f_1/\partial x_1 = a > 0$, $\partial f_1/\partial x_4 = b > 0$, $\partial f_2/\partial x_2 = c > 0$, $\partial f_2/\partial x_5 = d > 0$, $\partial h_3/\partial x_3 = e > 0$, $\partial h_3/\partial x_5 = -u < 0$, $\partial f_3/\partial x_4 = z > 0$, $\partial f_3/\partial x_5 = p > 0$, $\partial g_3/\partial x_3 = q > 0$, $\partial h_4/\partial x_4 = r > 0$, $\partial h_4/\partial x_5 = -s < 0$, $\partial g_5/\partial x_5 = t > 0$. Then, the system Jacobian matrix is

$$J(x) = J_0(x) - DI_5,$$

where I_5 is the 5×5 identity matrix and

$$J_0 = \begin{bmatrix} -k_1 c_x a & 0 & 0 & -k_1 c_x b & 0 \\ a & -c & 0 & b & -d \\ 0 & c & -e-q & z & d+u+p \\ -a & 0 & 2e & -b-2z-r & s-2p-2u \\ 0 & -c & 2e & r-2z & -d-2u-2p-s-t \end{bmatrix}.$$

The internal fluxes (f_i, g_i, h_i) are much higher than dilution due to growth (μx_i) and outflow (Dx_1, controlled to keep the bioreactor volume constant), and dominate the dynamics. Hence, we can make the following assumption.

Assumption 2: In the system in Table I, $D = \mu = 0$. ◇

If $D = \mu = 0$, the system admits a BDC-decomposition [4], [7], [8], [9], [14]: $J(x) = BD_x(x)C$, where

$$B = \begin{bmatrix} -k_1 c_x & -k_1 c_x & 0 & 0 & 0 & 0 & 0 & 0 & 0 & 0 & 0 & 0 & 0 \\ 1 & 1 & -1 & -1 & 0 & 0 & 0 & 0 & 0 & 0 & 0 & 0 & 0 \\ 0 & 0 & 1 & 1 & -1 & 1 & 1 & 1 & -1 & 0 & 0 & 0 & 0 \\ -1 & -1 & 0 & 0 & 2 & -2 & -2 & -2 & 0 & -1 & 1 & 0 & 1 \\ 0 & 0 & -1 & -1 & 2 & -2 & -2 & -2 & 0 & 1 & -1 & -1 & -1 \end{bmatrix},$$

$$C = \begin{bmatrix} 1 & 0 & 0 & 0 & 0 & 0 & 0 & 0 & 0 & 0 & 0 & 0 & 0 \\ 0 & 0 & 1 & 0 & 0 & 0 & 0 & 0 & 0 & 0 & 0 & 0 & 0 \\ 0 & 0 & 0 & 0 & 1 & 0 & 0 & 0 & 1 & 0 & 0 & 0 & 0 \\ 0 & 1 & 0 & 0 & 0 & 0 & 1 & 0 & 0 & 1 & 0 & 0 & 0 \\ 0 & 0 & 0 & 1 & 0 & 1 & 0 & 1 & 0 & 0 & 1 & 1 & 1 \end{bmatrix}^\top,$$

and $D_x(x) = \text{diag}\{a, b, c, d, e, u, z, p, q, r, s, t, v\}$ is the diagonal matrix that contains all the nonzero partial derivatives.

Then, the steady state can be proven to be unique.

Proposition 2: Under Assumptions 1 and 2, the system in Table I admits a unique steady state $\bar{x} \in \mathcal{B}$, which does not have zero components. □

Proof: When $D = \mu = 0$, the system Jacobian is J_0; $\det(-J_0) > 0$ structurally. Recall that, when $D = \mu = 0$, there cannot be steady-state vectors with zero components, and the system admits a BDC-decomposition. Therefore, structural non-singularity of the Jacobian implies that the steady state is unique, in view of [8, Theorem 3]. ■

C. Capability of oscillatory behaviour

Glycolytic oscillations are a well-investigated phenomenon in *S. cerevisiae* [2], [11], reported also in *E. coli* [22], [23], [31] and in human pancreatic beta-cells [33]. We show here that the proposed model has indeed the capability of generating oscillatory behaviours; in fact, the system is a strong candidate oscillator as defined in [5], [6].

In particular, consider the scenario in which, due to parameter variations, the Jacobian at the equilibrium has a transition to instability. A system is a strong candidate oscillator if any transition to instability occurs due to a pair of complex eigenvalues crossing the imaginary axis from the left to the right. Hence, exponential instability is excluded: if the system is driven to instability, it will necessarily give rise to sustained oscillations.

Proposition 3: Under Assumptions 1 and 2, the system in Table I is a strong candidate oscillator. □

Proof: If $D = \mu = 0$, the constant term of the characteristic polynomial $p(s)$ is $\det(-J_0)$, which is structurally positive: $p(0) > 0$. Hence, 0 cannot be an eigenvalue, and all transitions to instability (if any) must be due to complex eigenvalues whose real part becomes negative. ■

Therefore, either the unique steady state $\bar{x}$ is globally asymptotically stable, hence all trajectories $x(t)$ converge to $\bar{x}$ when $t \to \infty$, or the steady state is unstable, and sustained *glycolytic oscillations* will necessarily arise.

III. Steady-State Influences

In this section, we assume that the unique steady state is globally asymptotically stable. Then, upon a perturbation due to a constant input ε, after a transient the system will converge to a new steady state $\bar{x}_\varepsilon$. How does the new steady-state differ from the previous one? For systems admitting a BDC-decomposition, the sign of the variation between the old and the new steady-states can be computed based on the algorithm proposed in [14] (see also the extension [9] and the applications to biological systems in [13], [15], [16], [17]).

In particular, we can compute the structural steady-state influence matrix Σ_0 for the system with $D = \mu = 0$. The (i, j)-entry of Σ_0 represents the structural sign of the variation of the steady state of the ith variable due to a constant positive input added to the equation of the jth variable. This variation is always positive if $[\Sigma_0]_{ij} = 1$, negative if $[\Sigma_0]_{ij} = -1$, zero if $[\Sigma_0]_{ij} = 0$ (regardless of parameter values), while it depends on the parameter values if $[\Sigma_0]_{ij} =?$.

For the system in Table I, under Assumptions 1 and 2, the structural steady-state influence matrix computed with the algorithm in [14], based on the system BDC-decomposition, is

$$\Sigma_0 = \begin{bmatrix} ? & ? & -1 & -1 & ? \\ ? & ? & -1 & ? & -1 \\ 1 & 1 & 1 & 1 & 1 \\ ? & ? & 1 & 1 & ? \\ ? & ? & 1 & ? & 1 \end{bmatrix}. \quad (3)$$

Quite many influences (13 out of 25) are structurally signed, independent of parameter values. For instance, a persistent positive perturbation added to any of the equations will lead to an increase in the steady state of x_3, regardless of the system parameters. Also, a persistent positive perturbation added to $\dot{x}_3$ or $\dot{x}_5$ will always lead to a larger steady-state value of x_5. The first column is particularly interesting,

because it displays the effect of an abrupt increase in the value of the feeding input u_{GLC}^{feed}. The effect on x_5 is not sign-determined.

To get a more quantitative insight [15], [16], we can analyse the input-output sensitivity and give bounds for the components of $\Delta\bar{x}_\varepsilon/\varepsilon$, where $\Delta\bar{x}_\varepsilon$ is the variation in the steady state due to the applied perturbation ε, when the entries of matrix D_x in the BDC-decomposition are bounded as $0.1 \leq [D_x]_i \leq 10$. Then, when $k_1 = 16$ and $c_x = 0.0154$ $\mathrm{L}_{IC}/\mathrm{L}_{EC}$, the element-wise lower and upper bounds for Σ_0 can be computed as in [9]:

$$\begin{bmatrix} [-198123, 2271] & [-65866, 234] & [-88035, -0] & [-22289, -0] & [-22169, 491] \\ [-8208, 1034] & [-2730, 209] & [-3666, -0] & [-926, 197] & [-926, -0] \\ [0.2, 23] & [0.05, 10] & [0.05, 10] & [0.001, 5] & [0.001, 2] \\ [-22, 1981] & [2, 659] & [+0, 880] & [0.03, 223] & [-5, 222] \\ [-10, 83] & [-2, 27] & [+0, 37] & [-2, 9] & [-0.01, 9] \end{bmatrix}.$$

Consistently with the structural influence matrix, only the entries corresponding to '?' in Σ_0 have bounds with opposite signs (-0 and $+0$ denote extremely small negative and positive values, respectively). It can be noticed that the sign-indefinite intervals showing the sensitivity of x_5, $[ATP]$, are particularly tight, and this can explain the small variations in the energy charge even when the system is subject to drastic changes in u_{GLC}^{feed} and in the other state variables.

We can also compute the signed influence for randomly picked values of the parameters (in the interval $[0, 10]$ with uniform distribution) and average over the number of considered samples. With 10^7 samples, we obtain the matrix

$$\begin{bmatrix} 0.816 & -0.987 & -1 & -1 & -0.072 \\ 0.942 & 0.898 & -1 & -0.068 & -1 \\ 1 & 1 & 1 & 1 & 1 \\ -0 & 0.987 & 1 & 1 & -0.072 \\ -0 & -0.050 & 1 & 0.068 & 1 \end{bmatrix},$$

where, consistently with Σ_0, sign-definite entries are exactly equal to ± 1, while the value of sign-indefinite entries represents the prevalence of positive, or negative, signs. The variation of $\bar{x}_5$ due to perturbations on $\dot{x}_1$ appears to be positive or negative with very similar probability, and/or very often equal to zero.

IV. Simulation Results vs. Experimental Data

A. Periodic feeding: feast-famine perturbations

We compare here the behaviour of the proposed model in numerical simulations with previously unpublished experimental data collected through feast-famine experiments, used to mimic the dynamic conditions in large-scale bioreactors with a scale-down approach.

The experiments are carried out as shown in Fig. 1: *E. coli* cells are grown inside a bioreactor with a working volume of 1 L, as a pure culture. Glucose is used as the only substrate. The microorganisms oxidise glucose (electron donor) to provide energy for all the metabolic activities. Oxygen is also fed to the system (aerobic conditions) and acts as the electron acceptor. Glucose is fed to the reactor at a constant rate ($u_{GLC}^{feed} = 151$ mmol/L_{EC}/min) for 20 s and then feeding is stopped for 380 s. The procedure is repeated in successive cycles of 400 s. Due to this block-wise feeding, the cells experience a feast phase when glucose is still

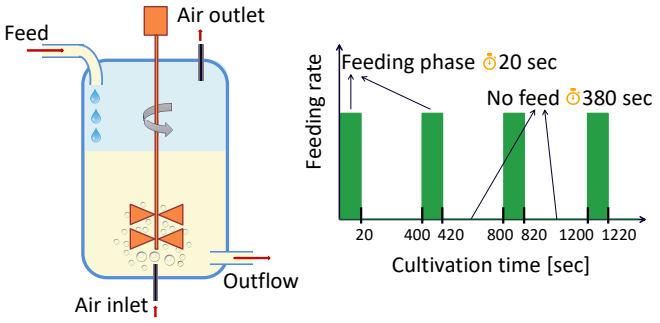

Fig. 1: Feast-famine perturbation experiments: glucose is fed at a constant rate for 20 s and then feeding is stopped for the next 380 s; the procedure is repeated in successive cycles of 400 s. Oxygen is constantly supplied, and samples are regularly taken to measure the concentration of metabolites.

significantly available (approx. the first 100 s) and a famine phase when practically all substrate is consumed. During the cultivations, samples for biomass and metabolome analysis are taken from the bioreactor.

During such a short famine phase, no biomass lysis is expected (namely, no cell death phenomena due to starvation).

For the numerical simulations, the parameters and the reaction rate functions for the system in Table I are chosen as follows: $k_1 = 16$ and $c_x = 0.0154$ $\mathrm{L}_{IC}/\mathrm{L}_{EC}$, while the reaction rate functions are chosen similarly to [22]:

$$f_1(x_1, x_4) = \frac{k_{11} x_1 x_4}{k_{12} + k_{13} x_4 + k_{14} x_1 + k_{15} x_1 x_4}, \quad (4)$$

$$f_2(x_2, x_5) = \frac{k_{21} x_5^\beta x_2^\alpha}{k_{22} + k_{23} x_5^\beta + x_2^\alpha}, \quad (5)$$

$$h_3(x_3, x_5) = \frac{k_{31} x_3}{1 + k_{33} x_3} \frac{1}{1 + x_5}, \quad (6)$$

$$f_3(x_4, x_5) = \frac{k_{32} x_4^\alpha}{k_{34} + x_4^\alpha} \frac{k_{36} x_5^\beta}{k_{35} + k_{36} x_5^\beta}, \quad (7)$$

$$g_3(x_3) = k_3 x_3, \quad (8)$$

$$h_4(x_4, x_5) = \frac{k_{41} x_4^\alpha}{k_{42} + k_{43} x_5^\gamma + x_4^\alpha}, \quad (9)$$

$$g_5(x_5) = k_5 x_5, \quad (10)$$

with parameters $k_{11} = 259740$ mmol/L_{IC}/min, $k_{12} = 1$ mmol^2/L_{IC}^2, $k_{13} = 1870$ mmol/L_{IC}, $k_{14} = 5911$ mmol/L_{IC}, $k_{15} = 0.5$, $k_{21} = 0.0088$ (mmol/L_{IC}=$^\beta$/min, $k_{22} = 12.76$ (mmol/L_{IC})$^\alpha$, $k_{23} = 2.5{\cdot}10^{-5}$ (mmol/L_{IC})$^{\alpha-\beta}$, $k_{31} = 6200$ mmol/L_{IC}/min, $k_{32} = 1000$ mmol/L_{IC}/min, $k_{33} = 10$ L_{IC}/mmol, $k_{34} = 5$ (mmol/L_{IC})$^\alpha$, $k_{35} = 10$ (mmol/L_{IC})$^\beta$, $k_{36} = 1.1{\cdot}10^{-5}$, $k_3 = 8$ 1/min, $k_{41} = 4.723$ mmol/L_{IC}/min, $k_{42} = 24$ (mmol/L_{IC})$^\alpha$, $k_{43} = 2.6 \cdot 10^{-6}$ (mmol/L_{IC})$^{\alpha-\gamma}$, $k_5 = 0.8$ 1/min, and exponents $\alpha = 2$, $\beta = 6$, $\gamma = 4$. Also, we consider $D = \mu = 1/60$ min^{-1}.

In the simulations, consistently with the experiments, $u_{GLC}^{feed} = 151$ mmol/L_{EC}/min for the first 20 s, and for the following 380 s $u_{GLC}^{feed} = 1$ mmol/L_{EC}/min (not zero to avoid numerical stability issues and also to represent storage mobilisation due to glycogen that, when $x_1 \approx 0$, produces glucose through a reaction that is not included in the model). The time evolution of the state variables $x_1 = [GLC]$,

$x_2 = [F6P]$, $x_3 = [FDP]$, $x_4 = [PEP]$, $x_5 = [ATP]$ is computed based on the dynamical system in Table I, integrated using the MATLAB function `ode23s`, while the concentrations of ADP and AMP are calculated based on Eqns. (1) and (2). The energy charge is then computed as

$$EC = \frac{[ATP] + 0.5[ADP]}{[ATP] + [ADP] + [AMP]}.$$

The initial conditions match those in the experiments: $x(0) = [0.25 \quad 0.1061 \quad 0.2122 \quad 6.19 \quad 6.72]^\top$, where the first concentration is in mmol/L$_{EC}$ while all the others are in mmol/L$_{IC}$. With the chosen functions and parameters, the system equilibrium is globally asymptotically stable.

Our proposed model is a phenomenological model based on the theory of chemical reaction networks, and has not been obtained by fitting the data, although of course the parameters have been chosen so as to qualitatively reproduce the experimental traces. Indeed, the results in Fig. 2 show that it is able to reproduce very well the trends of experimental data, and it gets also quite close to the actual values of the concentrations. Fig. 3, instead, shows how fluxes change during the simulation. As can be seen in Fig. 2, the concentration of glucose, x_1, has a peak in the first minute: it increases linearly during the feeding phase and then it abruptly decreases until, around 100 s, it reaches a very small value. The same happens to the concentrations of $F6P$, x_2, and of FDP, x_3, which are directly ($F6P$) or indirectly (FDP, via $F6P$) fed by the glucose peak, but abruptly decrease when glucose becomes scarce. On the contrary, the concentration of PEP, x_4, becomes suddenly higher when glucose is in short supply, because the reaction associated with f_1, which leads to a decrease in both GLC and PEP, almost stops occurring. In spite of the large and abrupt variations in the concentrations, and also in the fluxes shown in Fig. 3, the concentration of ATP, x_5, does not change significantly. Indeed, the amount of ATP is sustained in a twofold way, both through flux h_3, associated with x_3, and through flux h_4, associated with x_4. When x_3 abruptly decreases, x_4 abruptly increases, leading to a compensation that keeps x_5 almost constant. The same variations can be seen in the computed evolution of $[ADP]$ and $[AMP]$. Also the corresponding energy charge is practically constant, with values around 0.8, both for the experimental data and for the numerical simulation. Hence, the model reproduces the experimentally observed energy homeostasis.

Actually, in the simulated curves the variation in metabolite concentrations is often even larger than in experimental traces, and in spite of this the variation in EC is negligible. This shows that robustness is guaranteed anyways, even when the fluctuations are very large.

After the feeding is stopped, the system would reach a new steady state that is fully consistent with the predictions in Section III. However, periodic feeding prevents the system from reaching an actual steady state, and keeps it in a never-ending transient.

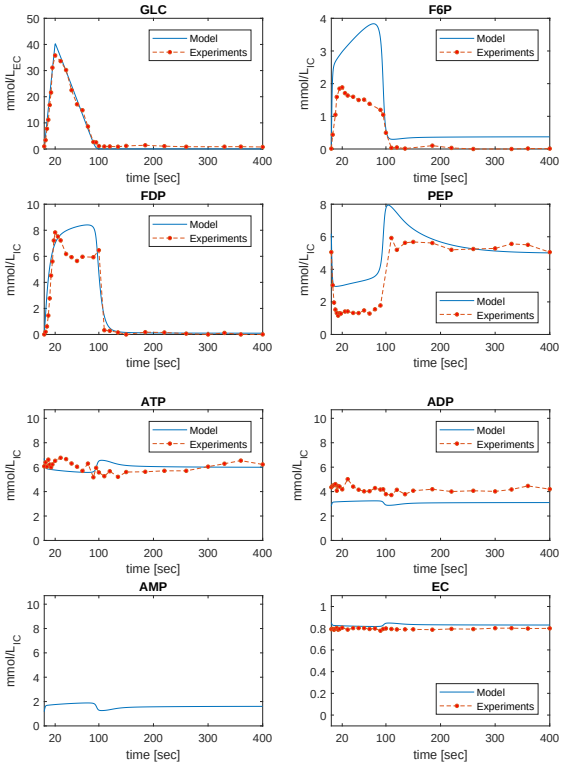

Fig. 2: Time evolution of the concentration of the metabolites: GLC, x_1; $F6P$, x_2; FDP, x_3; PEP, x_4; ATP, x_5; ADP, calculated; AMP, calculated; EC, computed energy charge. Glucose is externally fed for the initial 20 s and feeding is stopped for the following 380 s. Red dots show experimental data, while blue curves show the behaviour of the simulated model.

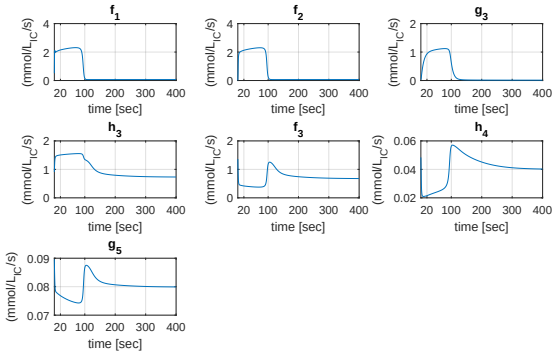

Fig. 3: Time evolution of the fluxes (reaction rate functions) in the simulated model, when glucose is externally fed for the initial 20 s and feeding is stopped for the following 380 s.

V. Concluding Discussion

We have presented a simple dynamical model for glycolysis in *E. coli* that predicts the experimentally observed energy homeostasis under dynamically changing environmental conditions, including feast-famine perturbations. Studying this phenomenon is particularly important for industrial fermentation in large-scale bioreactors, where the cells are subject to nutrient gradients that affect their metabolic responses.

A particularly interesting aspect revealed by this contribution is the importance of the role of glycogen (related to energy storage) in association with glycolysis, which is

worth a deeper analysis. Indeed, in our reduced model, including the additional reaction $FDP \xrightarrow{g_3} \emptyset$ (which is not biologically occurring in this form, but "represents" energy storage due to glycogen) was necessary to be able to satisfactorily reproduce the experimental traces and the observed energy homeostasis. This result suggests that the role of glycogen cannot be neglected, since it is key to explain the constant energy charge observed experimentally.

As previously mentioned, this low-order model takes into account the effect of storage just implicitly, by means of the reaction $FDP \xrightarrow{g_3} \emptyset$. However, the precise reaction occurring is $G6P + ATP \longrightarrow \text{glycogen} + ADP$ whenever the concentration of glucose is strictly positive (i.e., glucose is present and is consumed by the cells). Also, the reaction $\text{glycogen} \longrightarrow \text{glucose}$ occurs when glucose is absent: this effect has been implicitly taken into account in our model simulations by setting a very small, but not zero, feeding rate in the famine phase, to emulate the mobilisation of stored glycogen that occurs when the glucose concentration is zero. Explicitly including this storage accumulation/mobilisation effect in a higher-order model, by considering the concentration of $G6P$ and of glycogen as a state variable, could reduce the mismatch between the time evolution of the concentration of $F6P$ in the simulations and in the experiments and provide deeper insight into the observed phenomenon.

Other future research directions include using the new model presented here for control and optimisation of bioreactors, for instance to find the optimal feeding pattern that can maximise productivity and minimise waste, by-products and the needed amount of glucose to feed the microorganisms.

REFERENCES

[1] U. Alon, *An introduction to systems biology: design principles of biological circuits*. Chapman & Hall/CRC, 2006.

[2] M. Bier, B. Teusink, B. N. Kholodenko, H. V. Westerhoff, "Control analysis of glycolytic oscillations", *Biophysical Chemistry*, 62:15–24, 1996.

[3] F. Blanchini and E. Franco, "Structurally robust biological networks", *BMC Systems Biology*, 5(74), 2011.

[4] F. Blanchini, E. Franco, G. Giordano, "Determining the structural properties of a class of biological models", *Proc. 51st IEEE Conf. Decision and Control*, pp. 5505–5510, 2012.

[5] F. Blanchini, E. Franco, G. Giordano, "A structural classification of candidate oscillatory and multistationary biochemical systems", *Bulletin of Mathematical Biology*, 76(10):2542–2569, 2014.

[6] F. Blanchini, E. Franco, G. Giordano, "Structural conditions for oscillations and multistationarity in aggregate monotone systems", *Proc. 54th IEEE Conf. Decision and Control*, pp. 609–614, 2015.

[7] F. Blanchini and G. Giordano, "Piecewise-linear Lyapunov functions for structural stability of biochemical networks", *Automatica*, 50(10):2482–2493, 2014.

[8] F. Blanchini and G. Giordano, "Polyhedral Lyapunov functions structurally ensure global asymptotic stability of dynamical networks iff the Jacobian is non-singular", *Automatica*, 86(12):183–191, 2017.

[9] F. Blanchini and G. Giordano, "BDC-decomposition for global influence analysis", *IEEE Control Systems Letters*, 3(2):260–265, 2019.

[10] A. G. Chapman, L. Fall, and D. E. Atkinson, "Adenylate energy charge in *Escherichia coli* during growth and starvation", *Journal of Bacteriology*, pp. 1072–1086, 1971.

[11] F. A. Chandra, G. Buzi, and J. C. Doyle, "Glycolytic oscillations and limits on robust efficiency", *Science*, 333(6039):187–192, 2011.

[12] C. Chassagnole, N. Noisommit-Rizzi, J. W. Schmid, K. Mauch, M. Reuss, "Dynamic modeling of the central carbon metabolism of *Escherichia coli*", *Biotechnology and Bioengineering*, 79:53–73, 2002.

[13] G. Giordano, "CERT-mediated ceramide transfer is a structurally tunable flow-inducing mechanism with structural feed-forward loops", *Royal Society Open Science*, 5(6):180494, 2018.

[14] G. Giordano, C. Cuba Samaniego, E. Franco, and F. Blanchini, "Computing the structural influence matrix for biological systems", *Journal of Mathematical Biology*, 72(7):1927–1958, 2016.

[15] G. Giordano, C. Altafini, "Qualitative and quantitative responses to press perturbations in ecological networks", *Scientific Reports*, 7:11378, 2017.

[16] G. Giordano, C. Altafini, "Interaction sign patterns in biological networks: from qualitative to quantitative criteria", *Proc. 56th IEEE Conf. Decision and Control*, pp. 5348–5353, 2017.

[17] G. Giordano and E. Franco, "Negative feedback enables structurally signed steady-state influences in artificial biomolecular networks", *Proc. 55th IEEE Conf. Decision and Control*, pp. 3369–3374, 2016.

[18] J. H. van Heerden, M. T. Wortel, F. J. Bruggeman, J. J. Heijnen, Y. J. Bollen, R. Planque, J. Hulshof, T. G. O'Toole, S. A. Wahl, B. Teusink, "Fatal attraction in glycolysis: how *Saccharomyces cerevisiae* manages sudden transitions to high glucose", *Microbial Cell*, 1:103–106, 2014.

[19] H. Kitano, "Biological robustness", *Nature Reviews Genetics*, 5:826–837, 2004.

[20] A. Lapin, J. Schmid, and M. Reuss, "Modeling the dynamics of *E. coli* populations in the three-dimensional turbulent field of a stirred-tank bioreactor – A structured-segregated approach", *Chemical Engineering Science*, 61:4783–4797, 2006.

[21] A. R. Lara, H. Taymaz-Nikerel, M. R. Mashego, W. M. van Gulik, J. J. Heijnen, O. T. Ramirez, W. A. van Winden, "Fast dynamic response of the fermentative metabolism of Escherichia coli to aerobic and anaerobic glucose pulses", *Biotechnology and Bioengineering*, 104:1153–1161, 2009.

[22] G. Maria, "In silico derivation of a reduced kinetic model for stationary or oscillating glycolysis in *Escherichia coli* bacterium", *Chemical and Biochemical Engineering Quarterly*, 28:509–529, 2014.

[23] G. Maria, C. L. Gijiu, C. Maria, C. Tociu, "Interference of the oscillating glycolysis with the oscillating tryptophan synthesis in the *E. coli* cells", *Computers & Chemical Engineering*, 108:395–407, 2018.

[24] D. Richeson and J. Wiseman, "Addendum to: D. Richeson and J. Wiseman, "A fixed point theorem for bounded dynamical systems", Illinois J. Math., 46(2):491–495, 2002", *Illinois Journal of Mathematics*, 48(3):1079–1080, 2004.

[25] G. Shinar and M. Feinberg, "Structural sources of robustness in biochemical reaction networks", *Science*, 327:1389–1391, 2010.

[26] R. Srzednicki, "On rest points of dynamical systems", *Fundamenta Mathematicae*, 126(1):69–81, 1985.

[27] R. Steuer, S. Waldherr, V. Sourjik, M. Kollmann, "Robust signal processing in living cells", *PLoS Computational Biology*, 7:e1002218, 2011.

[28] C. Suarez-Mendez, C. Ras, S. A. Wahl, "Metabolic adjustment upon repetitive substrate perturbations using dynamic 13 C-tracing in yeast", *Microbial Cell Factories*, 16:161, 2017.

[29] V. Takhaveev and M. Heinemann, "Metabolic heterogeneity in clonal microbial populations", *Current Opinion in Microbiology*, 45:30–38, 2018.

[30] H. Taymaz-Nikerel, M. De Mey, G. Baart, J. Maertens, J. J. Heijnen, W. van Gulik, "Changes in substrate availability in *Escherichia coli* lead to rapid metabolite, flux and growth rate responses", *Metabolic Engineering*, 16:115–129, 2013.

[31] Y. Termonia, J. Ross, "Oscillations and control features in glycolysis: numerical analysis of a comprehensive model", *Proceedings of the National Academy of Sciences of the United States of America*, 78:2952–2956, 1981.

[32] E. Vasilakou, D. Machado, A. Theorell, I. Rocha, K. Noh, M. Oldiges, S. A. Wahl, "Current state and challenges for dynamic metabolic modeling", *Current Opinion in Microbiology*, 33:97–104, 2016.

[33] P. O. Westermark and A. Lansner, "A model of phosphofructokinase and glycolytic oscillations in the pancreatic Beta-cell", *Biophysical Journal*, 85:126–139, 2003.